

Dynamics of Nonequilibrium Membrane Bud Formation

Pierre Sens*

Institut Charles Sadron, 6 rue Boussingault, 67083 Strasbourg, France
and Institut Curie, section recherche, 11 rue Pierre et Marie Curie, 75231 Paris Cedex 05, France
 (Received 8 April 2003; published 2 September 2004; publisher error corrected 3 September 2004)

The dynamical response of a lipid membrane to a *local* perturbation of its molecular symmetry is investigated theoretically. A density asymmetry between the two membrane leaflets is predominantly released by in-plane lipid diffusion or membrane curvature, depending upon the spatial extent of the perturbation. It may result in the formation of nonequilibrium structures (buds), for which a dynamical size selection is observed. A preferred size in the μm range is predicted, as a signature of the crossover between membrane and solvent dominated dynamical membrane response.

DOI: 10.1103/PhysRevLett.93.108103

PACS numbers: 87.16.Dg, 67.40.Fd

The formation of small membrane structures (vesicles or tubules, etc.) is required for most intercellular and intracellular transports in biological cells [1]. While important progress has been made in the identification of key membrane proteins, recent work has focused on the lipid molecules themselves [2]. Of particular interest is the lipid translocation by specific enzymes (flippases), and the membrane morphological changes they trigger [3,4]. From a physical point of view, the formation of a bud from a fluid membrane has mostly been considered as the result of phase separation in mixed membranes [5], or as a global shape transition of closed membranes due to geometric frustration [6]. The final membrane conformation then corresponds to a global equilibrium and is not expected to depend upon dynamics [7].

Small invaginations of the plasma membrane of biological cells should, however, result from localized perturbations rather than from global changes at the scale of the cell. This Letter presents a theory for the dynamics of relaxation of one such local perturbation: a local membrane asymmetry, created by a sudden flip of a number of lipids from one leaflet of the bilayer to the other. This situation is of fundamental interest, as it may result in the formation of nonequilibrium membrane structures. The model also seeks to mimic experiments where the local perturbation of a giant vesicle ($\sim 100 \mu\text{m}$) by adsorption of DNA molecules results in the production of small dynamical vesicles ($\sim \mu\text{m}$) with their membrane packed with adsorbed DNA [8].

It is shown here that the local membrane perturbation introduced by lipid translocation [stretching of the depleted monolayer and compression of the enriched one (Fig. 1)] may be released both by opposite monolayer flows, leading to a diffusion of the perturbation [Fig. 1(a)] or by membrane curvature [Fig. 1(b)]. While the former mechanism potentially leads to a vanishingly small energy, the faster of the two processes will control the membrane relaxation. It is shown below that large-scale-membrane curvature is hindered by bulk flow, while small-scale-membrane curvature is slowed by membrane flow. The crossover between these two regimes defines a

critical dynamical length scale $\lambda_D \sim 1 \mu\text{m}$ in water and $\sim 100 \text{ nm}$ in the more viscous inner cellular environment, at which the perturbation is optimally converted into a transient membrane curvature, and fully formed membrane buds are most likely to be observed.

Lipid membranes are self-assembled fluid bilayers. Their equilibrium properties such as lipid density ϕ_0 and membrane thickness $2d$ ($\sim 4 \text{ nm}$) result from a balance of the hydrophobic attractions between the lipid tails by steric or electrostatic repulsions [9]. Deviation from the optimal density costs an elastic energy (*per monolayer*, per unit area) $K_s(\phi - \phi_0)^2/(2\phi_0^2)$, with a large stretching modulus $K_s \sim 25k_B T/\text{nm}^2$ [10] ($k_B T$ is the thermal energy). The membrane bending energy $\kappa C^2/2$ involves the local membrane curvature C and a fairly small bending modulus $\kappa \sim 25k_B T$. Noting the outer (+) and inner (−) monolayer densities (at the midplane) ψ_{\pm} (with $\phi_{\pm} = \psi_{\pm}(1 \mp dC)$), the membrane elastic energy is best expressed in terms of the local average dilation $\bar{\rho} \equiv \frac{\psi_+ + \psi_-}{2\psi_0} - 1$ and the dilation difference between the monolayers $\rho \equiv \frac{\psi_+ - \psi_-}{2\psi_0}$ [9]:

$$\mathcal{F}_{\text{elast}} = \int dS \left[K_s(\rho - dC)^2 + K_s \bar{\rho}^2 + \frac{\kappa}{2} C^2 \right]. \quad (1)$$

Bending a symmetrical bilayer ($\rho = 0$) involves a bending modulus $\kappa + 2K_s d^2 \sim 200k_B T$. It is reduced to κ in fluid membranes since the monolayer densities can adjust to $\rho = dC$. The (small) “bending ratio” of these two quantities $\epsilon \equiv \kappa/(2K_s d^2)$ will prove important later.

Here, we assume that some fraction ρ_0 of the lipid is suddenly flipped from the “down” to the “up” monolayer

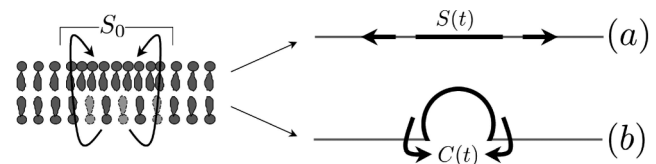


FIG. 1. Relaxation of a membrane asymmetry (a) in-plane diffusion and (b) membrane curvature.

over an area S_0 (Fig. 1). For simplicity the membrane bears no global surface tension ($\bar{\rho} = 0$). Lipid flow toward the stretched region of the down monolayer and away from the compressed region of the up monolayer diffuse the perturbation over the membrane [Fig. 1(a)]. Concomitantly, the compression extension creates a bending torque leading to membrane curvature [Fig. 1(b)]. Diffusion of the perturbation is limited by the sliding friction between monolayers, while membrane curvature is limited by membrane and solvent viscous dissipation.

Local balance between elastic and dissipative forces yields local equations for the evolution of the membrane shape. Such equations exist for small membrane deformations [9] but are hardly tractable for large deformations. In consequence, we take a simpler approach where the perturbed membrane [of area $S(t)$] is parametrized by a spherical cap of constant curvature $C(t)$ and constant dilation difference $\rho(t)$, connected to an unperturbed membrane with $C = \rho = 0$ [Fig. 1(b)]. This approximation disregards the existence of a connecting neck between the bud and the flat membrane, the stability of which is not well understood physically and is beyond the scope of this work. In the biological context, the scission of vesicles from membranes often requires the action of specific fusion proteins [11].

Spontaneous lipid flip flop between the two monolayers is very unlikely over the evolution time, which imposes the conservation of asymmetry $S(t)\rho(t) = S_0\rho_0$. The stretching stress in the perturbed region is released when $C = \rho/d$ [Eq. (1)]. The membrane geometry is described by a *budding parameter*, equal to unity for closed buds:

$$0 < B_d \equiv \frac{SC^2}{16\pi} < B_d^{(0)}, \quad (2)$$

where $B_d^{(0)} = S_0\rho_0^2/(16\pi d^2)$ corresponds to a situation where the perturbation is entirely converted into curvature, without diffusion along the membrane. As we will see, B_d is always much smaller than $B_d^{(0)}$, and the optimal conversion of perturbation into curvature is observed for a particular dynamical length scale $\sqrt{S_0} \sim \lambda_D$ [Eq. (8)].

Dynamical equations for the two independent variables S and C are obtained using a Lagrangian description [12], where elastic and dissipative “forces” are calculated from the variation of the elastic energy $\mathcal{F}_{\text{elast}}[\{\rho, C\}]$, and the energy dissipated per unit time $\mathcal{P}_{\text{diss}}$:

$$\frac{\partial \mathcal{F}_{\text{elast}}}{\partial \{\rho, C\}} + \frac{\partial \mathcal{P}_{\text{diss}}}{\partial \{d_t \rho, d_t C\}} = 0. \quad (3)$$

Variation with ρ accounts for the migration of lipid molecules under a gradient of chemical potential, and variation with C describes the membrane deformation due to the bending torque.

The three sources of dissipation involve three constitutive parameters. The viscosities of the solvent η ($\approx 10^{-3}$ N/m² for water) and of the membrane μ_m

($\approx 10^{-9}$ Ns/m) couple to gradients of bulk and membrane velocity fields \mathbf{v} into viscous shear stresses $\sigma_{ij} = \eta(\partial_j v_i + \partial_i v_j)$ [13]. An interlayer friction parameter b_m ($\approx 10^8$ Ns/m³) couples to the velocity difference δv between the two monolayers in relative motion [10]. Note that μ_m and b_m are related to the membrane (three-dimensional) viscosity η_m by the scaling relations $\eta_m \sim \mu_m/d \sim b_m d$, where the membrane viscosity is typically a thousand times the viscosity of water [14]. The total dissipation is $\mathcal{P}_{\text{diss}} = \mathcal{P}_{b_m} + \mathcal{P}_{\mu_m} + \mathcal{P}_\eta$, with

$$\mathcal{P}_{b_m} = \frac{b_m}{2} \int dS \delta v^2; \quad \mathcal{P}_\eta = \frac{1}{2\eta} \int dV \sum_{ij} (\sigma_{ij})^2. \quad (4)$$

The membrane viscous dissipation \mathcal{P}_{μ_m} is obtained by substituting μ_m to η in \mathcal{P}_η and integrating over the membrane surface instead of the volume.

The three contributions to the energy dissipation are calculated as follows (see [15] for a related calculation). The bud volume V and neck aperture L satisfy $V = \frac{S^2 C}{8\pi} \times (1 - \frac{2}{3} B_d)$, $\pi L^2 = S(1 - B_d)$. The curvilinear, radial, and spherical coordinate systems defined in Fig. 2 are used to parametrize flows in the curved and flat part of the membrane, and in the bulk, respectively. The differential monolayer velocity δv is present in the perturbed part of the membrane. It is axisymmetrical and relaxes the concentration difference ρ according to the continuity relation [9] $\nabla_c \cdot \delta \mathbf{v} = -\dot{\rho}$, or $\delta v = -4\dot{\rho}(1 - \cos\Psi)/(C \sin\Psi)$ (where the dot represents a time derivative, ∇_c is the curvilinear gradient along the membrane, and Ψ is defined in Fig. 2(a)). The dissipated energy due to intermonolayer friction is calculated from Eq. (4):

$$\mathcal{P}_{b_m} = \frac{b_m}{4\pi} S^2 \dot{\rho}^2 \left[\frac{2}{B_d} \left(\log \frac{1}{1 - B_d} - B_d \right) \right]. \quad (5)$$

We assume incompressible flows in the membrane and the surrounding fluid. Most of the membrane flow comes from bringing the membrane area from the flat membrane into the bud. The flow matches the variation of the area $\Delta S = S - \pi L^2 = SB_d$ and corresponds to a radial velocity field $v_{\text{membr}} = -d_t(\Delta S)/(2\pi l)$ (where l is defined in Fig. 2(b)). The main source of solvent flow comes from the variation \dot{V} of the volume inside the bud, which imposes a flow going through the circular neck of radius L . In the spherical coordinate system [Fig. 2(c)], the velocity field is radial and has the expression [13] $v_{\text{bulk}} = \frac{3\dot{V}}{2\pi r^2} \cos^2\theta$. The bulk and membrane viscous dissipation are obtained from Eq. (4):

$$\mathcal{P}_\eta = \frac{22}{5} \eta \frac{(\dot{V})^2}{\pi L^3}; \quad \mathcal{P}_{\mu_m} = \mu_m \frac{[d_t(\Delta S)]^2}{\pi L^2}. \quad (6)$$

Viscous dissipation in the solvent occurs on both sides of the membrane. \mathcal{P}_η in Eq. (6) is for the fluid entering the bud. For the fluid expelled by the bud, the neck size L is approximately replaced by the bud radius $2/C$ beyond the hemispherical bud. Extra sources of dissipation, such as

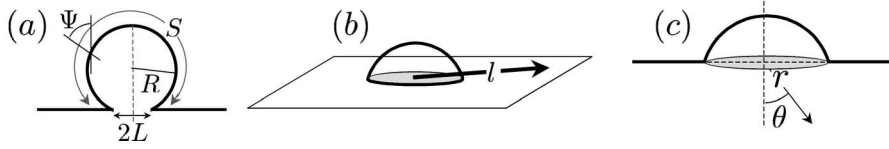


FIG. 2. Parametrization for the membrane shape surface S , curvature $C = 2/R$, and radius of the neck L , and the various coordinate systems used to derive the dissipation.

the solvent flow inside the bud, and membrane shear flow in the curving membrane, have been checked not to modify the membrane relaxation qualitatively.

The evolution of S and C is entirely determined by Eqs. (1), (3), (5), and (6). Notwithstanding the simple assumptions for the membrane shape, these equations [Eqs. (9) and (10)] are fairly complex and have to be dealt with numerically. In the limit of small deformations $B_d \ll 1$, all equations may be linearized, and membrane viscous dissipation is negligible. The membrane asymmetry relaxes via diffusion: $S\dot{\rho} = -D(\rho - dC)$ with the diffusion coefficient D and characteristic relaxation time t_0 (~ 0.1 ms for $S_0 \sim \mu\text{m}^2$):

$$D \equiv 4\pi \frac{K_s}{b_m} \sim 10^{-8} \text{ m}^2/\text{s}; \quad t_0 \equiv \frac{S_0}{D}. \quad (7)$$

The influence of the perturbation length scale S_0 is em-

$$\left[\sqrt{\bar{S}_0} \frac{(1 - 2B_d)^2}{(1 - B_d)^{3/2}} \left(s^{5/2} \dot{c} + 2 \frac{(1 - B_d)}{(1 - 2B_d)} s^{3/2} c \dot{s} \right) \right] + \left(\frac{\mu_m}{b_m d^2} \right) \frac{B_d}{(1 - B_d)} (s^2 \dot{c} + s c \dot{s}) = [1 - (1 + \epsilon) s c]. \quad (10)$$

The driving forces for diffusion and membrane deformation (right-hand side of the above equations) both show the competition between increases of s and c .

At short time ($s \sim 1$ and $c \ll 1$), the evolution is given by $\dot{s} \sim 1$ and $\dot{c} \sim 1/\sqrt{\bar{S}_0}$. For $\bar{S}_0 < 1$, membrane curvature moves little solvent and occurs faster than diffusion. On the other hand, membrane deformation is slow for $\bar{S}_0 > 1$. For larger deformation however, the membrane viscosity comes into play. It is characterized by a single parameter $\alpha_m \equiv \mu_m/(b_m d^2)$ (typically slightly larger than unity [14]) and becomes important for small scale perturbations ($\sqrt{\bar{S}_0} \lesssim \alpha_m B_d \sqrt{1 - B_d}/(1 - 2B_d)^2$).

Figure 3 shows typical solutions of Eqs. (9) and (10). The budding parameter B_d rises from zero to a maximum value $B_d^{(\text{max})}$ over a time t_{growth} ; then it decays slowly over a larger time t_{decay} . Indeed, the driving force for diffusion [(1 - sc), Eq. (9)] vanishes only upon complete release of the stretching stress ($C = \rho/d$), while the driving force for membrane deformation [(1 - (1 + ϵ) sc), Eq. (10)] vanishes for smaller deformation due to membrane bending rigidity [$\epsilon \equiv \kappa/(2K_s d^2)$]. The ratio $B_d^{(\text{max})}/B_d^{(0)}$ gives the fraction of the initial perturbation that can be transiently converted into membrane deformation. For small deformations, the rise occurs over the linear evolution time $t_{\text{growth}} \sim t_0$, and the decay, mostly driven by bending rigidity, is of

phasized by using dimensionless variables for area, curvature, and time: ($s \equiv S/S_0$, $c \equiv dC/\rho_0$, and $\tau \equiv t/t_0$) with $B_d = B_d^{(0)} s c^2$ [see Eq. (2)]. Balancing the curvature forces lead to an equation for C . The interplay between membrane and solvent dissipation defines a characteristic length scale $\lambda_D \sim b d^2/\eta$ [9,10,16], to which the size of the perturbation should be compared.

$$\lambda_D \equiv \frac{20\sqrt{\pi} b d^2}{11 \eta}; \quad \bar{S}_0 \equiv \frac{S_0}{\lambda_D^2}. \quad (8)$$

This length scale λ_D is of order 1 μm in water and is much shorter (~ 100 nm) in biological cells, since the cytosol can be very viscous.

Expressed in the dimensionless variables, the set of equations reads [17]

$$\left[\frac{2}{B_d^2} \left(\log \frac{1}{1 - B_d} - B_d \right) \right] \dot{s} = (1 - s c), \quad (9)$$

order $t_{\text{decay}} \sim t_0/\epsilon$. As shown in Fig. 3, the evolution is much slower in the nonlinear regime.

Equations (9) and (10) determine the full dynamics of the membrane deformation. Here we concentrate on the following question: What is the amount of initial perturbation needed to transiently produce well-formed buds before it diffuses away? Figure 4 shows the value of the initial density of flips ρ_0 and of the initial perturbation $B_d^{(0)}$ needed to obtain a given maximum of the budding parameter $B_d^{(\text{max})}$. It illustrates the importance of the perturbation length scale S_0 in the nontrivial competition between membrane and solvent dynamics.

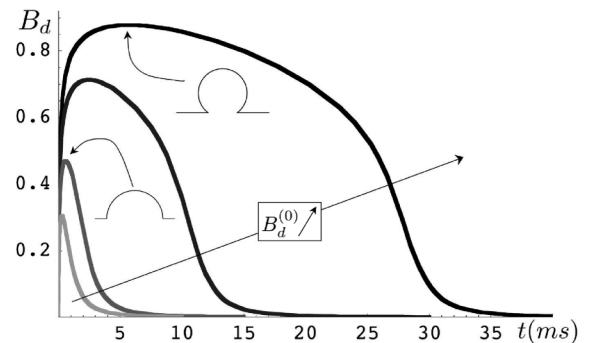


FIG. 3. Time evolution of the budding parameter $B_d \propto SC^2$ for initial perturbations ranging from $B_d^{(0)} = 3$ (light gray) to 6 (black) (with $S_0 = \lambda_D = 1 \mu\text{m}$; $\epsilon = 0.2$; $\alpha_m = 3$).

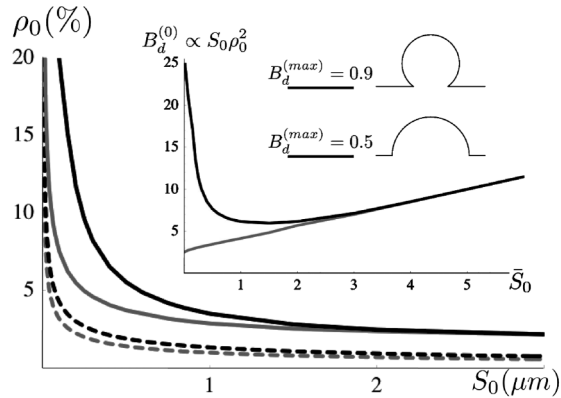


FIG. 4. Density of flips ρ_0 needed to reach hemispherical (gray line) and nearly completed buds [$B_d^{(\max)} = 0.9$ (black line)], as a function of the initial extension S_0 . The dashed lines are in the absence of lateral diffusion, when all the perturbation is converted into membrane deformation. The inset shows the initial perturbation $B_d^{(0)}$ needed to reach the same levels of deformation ($\epsilon = 0.2$; $\alpha_m = 3$; $\lambda_D = 1 \mu\text{m}$).

Extended perturbations ($\bar{S}_0 > 1$) are dominated by solvent dissipation. Interestingly in this limit, the diffusion of the perturbation (increase of S) promotes bud closure (increase of C) to minimize the dissipation associated to the variation of the bud volume [$\dot{V} = 0$ when $S\dot{C}(2B_d - 1) = 2C\dot{S}(1 - B_d)$]. In consequence, a bud is likely to close if it reaches the hemispherical shape, and the solid curves in Fig. 4 superimpose for $\bar{S}_0 \gg 1$. Surprisingly, the density ρ_0 needed to reach a given membrane deformation tends to a constant value for $\bar{S}_0 \gg 1$, so that the total mass of the perturbation $\rho_0 S_0$ linearly increases. In the small extension limit $\bar{S}_0 < 1$, large deformations require very large perturbations because the viscous flow in the membrane dissipates a lot of energy. The effect of nonlinearity and membrane viscosity is best seen by comparing the gray and black curves in the inset of Fig. 4.

Figure 4 shows that for large deformation ($B_d^{(\max)} > 0.5$), there is an optimal length scale at which the conversion of the initial perturbation into membrane deformation is the most efficient (a minimum in the inset curve). This length scale is purely dictated by dynamics, and it can be shown numerically that it is of order $\lambda_D \alpha_m / 2 \sim \lambda_D$. Mature buds have the best chances to be produced at this particular length scale, as the maximum membrane deformation $B_d^{(\max)}$ is closest to the optimal one $B_d^{(0)}$. Interestingly, the DNA-induced budding of giant vesicles [8] results in endosomes of size close to this optimal dynamical size in water ($\sim \mu\text{m}$). It is hazardous to make a more quantitative comparison with these experiments, since a number of other factors such as the kinetics of DNA adsorption certainly influences the formation of buds, but it is one prediction of the present work that the bud size can be altered by changing the solvent viscosity.

According to Fig. 4, well-formed buds with $B_d = 0.9$ require flipping only $\rho_0 \sim 3.5\%$ lipids over an area $S_0 \sim$

$1 \mu\text{m}^2$ (for $\lambda_D = 1 \mu\text{m}$), while it necessitates $\rho_0 = 35\%$ for $S_0 \sim (200 \text{ nm})^2$. This amounts to flipping about 10^5 molecules in both cases. The flips need not being perfectly synchronized, as successive events may act cooperatively if they are separated by a time lag shorter than the perturbation decay time t_{decay} seen in Fig. 3.

In conclusion, nonlinear dynamical equations for the formation of budlike invaginations in fluid membranes have been derived and applied to the relaxation of a localized perturbation of the up/down symmetry of lipid bilayers. Nonequilibrium buds may be produced provided that relaxation by membrane curvature occurs faster than the diffusion of the perturbation along the membrane. The membrane response critically depends upon the extension of the initial perturbation, which determines whether the membrane deformation is limited by membrane or solvent dynamics. Bud formation is most likely at the crossover between the two regimes.

I thank Albert Johner for many enjoyable discussions.

*Electronic address: Pierre.Sens@curie.fr

- [1] B. Alberts, D. Bray, J. Lewis, M. Raff, K. Roberts, and J. Watson, *Molecular Biology of the Cell* (Garland, New York, 1994).
- [2] R. Golsteyn, *Trends Cell Biol.* **10**, 9 (2000).
- [3] E. Farge, D. M. Ojcius, A. Subtil, and A. Dautry-Varsat, *Am. J. Physiol. Cell Physiol.* **276**, C725 (1999); P. F. Devaux, *Biochimie* **82**, 497 (2000).
- [4] E. M. Bevers, P. Comfurius, D. W. Dekkers, and R. F. Zwaal, *Biochim. Biophys. Acta* **1439**, 317 (1999).
- [5] D. D. Lasic, U. R. Joannic, B. C. Keller, P. M. Frederik, L. Auvray, *Adv. Colloid Interface Sci.* **89**, 337 (2001); F. Julicher and R. Lipowsky, *Phys. Rev. Lett.* **70**, 2964 (1993).
- [6] H.-G. Döbereiner, E. Evans, M. Kraus, U. Seifert, and M. Wortis, *Phys. Rev. E* **55**, 4458 (1997).
- [7] P. B. Sunil Kumar and M. Rao, *Phys. Rev. Lett.* **80**, 2489 (1998); P. B. Sunil Kumar, G. Gompper, and R. Lipowsky, *Phys. Rev. Lett.* **86**, 3911 (2001).
- [8] M. I. Angelova and N. H. Tsoneva, *Eur. Biophys. J.* **28**, 142 (1999).
- [9] U. Seifert and S. A. Langer, *Eur. Lett.* **23**, 71 (1993).
- [10] E. Evans and A. Yeung, *Chem. Phys. Lipids* **73**, 39 (1994).
- [11] R. Jahn and H. Grubmüller, *Curr. Opin. Cell Biology.* **14**, 488 (2002).
- [12] H. Goldstein, *Classical Mechanics* (Addison-Wesley, Reading, MA, 1980), 2nd ed.
- [13] J. Happel and H. Brenner, *Low Reynolds Number Hydrodynamics* (Kluwer, Dordrecht, 1991).
- [14] R. Dimova, B. Pouligny, and C. Dietrich, *Biophys. J.* **79**, 340 (2000).
- [15] T. M. Fisher, *Phys. Rev. E* **50**, 4156 (1994).
- [16] P. Sens and H. Isambert, *Phys. Rev. Lett.* **88**, 128102 (2002).
- [17] Linear expansion of Eqs. (9) and (10) reproduce the results of Ref. [9] for small deformation, which validates the present parametrization of the membrane shape.